JOURNAL OF MATERIALS SCIENCE 30 (1995) 1689–1697

Modelling the properties of rubber-modified epoxy polymers

F. J. GUILD
Department of Materials Science and Engineering, University of Surrey, Guildford, Surrey, GU2 5XH, UK

A. J. KINLOCH
Department of Mechanical Engineering, Imperial College of Science, Technology and Medicine, Exhibition Rd, London, SW7 2BX, UK

A finite-element model for rubber particles in a polymeric matrix has recently been proposed which is based upon a collection of spheres, each consisting of a sphere of rubber surrounded by an annulus of matrix. We have used this model to investigate in detail the stress distributions in and around a rubber particle, or a void, in a matrix of epoxy polymer. We have deduced the bulk modulus of the rubber-toughened epoxy and considered the implications of the stress distributions on the observed toughening micromechanisms. Of particular concern has been the effects of the volume fraction and the properties of the rubber phase.

1. Introduction

Epoxy resins are frequently toughened by the addition of rubber particles and such two-phase polymers are important materials both as structural adhesives and as matrices for fibre- and particulate-composites [1–6]. The rubber particles are typically about 0.5 to 5 μm in diameter and are present at a volume fraction of between 5 and 30 %. The presence of these particles greatly increases the toughness of the epoxy polymer, but does not significantly decrease other important properties of the material. The mechanisms of toughening in these rubber-toughened epoxy polymers is therefore an important area for both experimental studies and predictive modelling. In particular, the use of predictive modelling as an investigative tool can lead to both the elucidation of experimental observations and suggestions for possible routes to improved materials.

An important requirement in establishing a predictive model is to identify the micromechanisms which lead to the improvement in the toughness of the cross-linked epoxy polymer when it contains a dispersed phase of rubber particles. Two important toughening mechanisms have been identified for such two-phase materials. The first is localized shear yielding, or shear banding, which occurs between rubber particles at an angle of approximately $\pm 45°$ to the direction of the maximum principal tensile stress [1–6]. Due to the large number of particles involved, the volume of thermoset matrix material which can undergo plastic yielding is effectively increased compared to the single-phase polymer. Consequently, far more irreversible energy dissipation is involved and the toughness of the material is improved. The second mechanism is the internal cavitation, or interfacial debonding, of the rubbery particles, which then may enable the subsequent growth of these voids by plastic deformation of the epoxy matrix [5–7]. The importance of this mechanism is that the irreversible hole-growth process of the epoxy matrix also dissipates energy and so contributes to the enhanced fracture toughness.

The above mechanisms are triggered by the different types of stress concentrations which act within the overall stress field in the two-phase material. For example, the initiation and growth of the shear bands are largely governed by the concentration of von Mises (deviatoric) stress in the matrix, whilst the cavitation, or interfacial debonding, of the rubber particle is largely controlled by the hydrostatic (dilatational) tensile stresses which are acting. Obviously, a basic step in the development of a predictive model is, therefore, to map the distribution of stresses which are acting in and around the rubber particles as a function of the volume fraction of the rubber phase and the properties of the rubber particles and epoxy matrix.

To analyse accurately the stress field, it is necessary to employ numerical methods such as the finite-element method. The first such study of rubber-modified polymers, which used an elastic analysis, was reported by Broutman and Panizza [8]. They simplified the two-phase material into an assembly of axisymmetric cylindrical cells. Their study revealed that the maximum direct and shear stresses were located at the equator of the particle, indicating that yielding of the matrix would initiate from this point. They also found that the stress concentration increased in size as the volume fraction of rubbery particles was increased. Later, Agarwal and Broutman [9] developed

0022–2461

a three-dimensional model assuming a regular packing of the rubbery particles. The results from using such a model were compared with the previous results obtained from employing the axisymmetric analysis. The two sets of results were found to agree well when presented as a function of inter-particle spacing. Since a three-dimensional analysis was more complicated, and more costly in terms of computer resources, the authors subsequently concluded that the axisymmetric model could be used without a significant loss in accuracy.

In a more recent study, a spatial statistical technique, developed by Davy and Guild [10], was incorporated into the axisymmetric model by Guild and Young [11] to study the influence of particle distribution on stress states around rubber particles. Their study suggested that particle distribution does not significantly change the calculated stress states around rubber particles when the rubbery volume fraction is below 0.3, which is usually the upper limit in rubber-toughened epoxy polymers [1]. In a later paper Guild *et al.* [12] again used the axisymmetric model, but modelled the effect of particle morphology on the stress distributions in the material.

The above-mentioned analyses were essentially elastic in nature. However, Huang and Kinloch [5, 6] have developed a two-dimensional plane-strain model to analyse the stress fields around the dispersed rubbery particles in multiphase rubber-modified epoxy polymers where the epoxy matrix was modelled as either an elastic or elastic-plastic material. Their work revealed that the plane-strain model predicted higher stress concentrations within the glassy polymeric matrix than the axisymmetric model. Furthermore, they successfully applied their model to simulate the initiation and growth of the localized shear bands in the epoxy matrix which were initiated around rubber particles or voids. However, since this earlier model developed by Huang and Kinloch was essentially two-dimensional in nature, it could not accurately model the mechanism of cavitation/debonding of the rubber particle and the subsequent plastic hole-growth in the epoxy matrix. Their finite-element analysis studies were also limited by the fact that their code was unable to incorporate relatively high values of the Poisson's ratio, ν, of the rubber particles. Therefore, these authors were forced to combine the finite-element analysis with an analytical model in order to predict the fracture energy, G_{Ic}, of the rubber-modified epoxy. This work emphasized the need for better, and more realistic, finite-element analysis models.

More recently, Guild and Kinloch [13] have developed a more accurate material model for analysing the stress distribution around the rubber particles. This model is based upon the idea of analysing a representative cell of the material. The use of a representative cell for finite-element analysis is based on the concept that the interactions of neighbouring particles on the given particle are not directional; the overall effect is an 'average' arising from all the neighbouring particles. This assumption is reasonable for the low range of volume fractions used in this material. Thus, the overall material can be divided into cells, each containing a single rubber sphere with a surrounding matrix of epoxy polymer. The boundary of a given cell is the region of the matrix closer to that particle than any other. These cells are the Voroni cells; for a random distribution of particles the distribution of cell sizes can be calculated (Davy and Guild [10]). On 'average' the shape of the Voroni cell is spherical. Thus, the overall material model is a collection of spherical cells of different sizes, each containing a single rubber sphere. Strictly, any overall property for the material should be obtained by summing the contributions from the different cell sizes. This summing may be carried out by application of a 'dispersion factor' to the property value found for the cell describing the overall volume fraction. It should be noted that the correct use of this idea of a representative cell can only be achieved by analysis of a spherical cell. The results presented in the present paper have been obtained for the spherical cell which describes the overall volume fraction. The application of the spatial statistical model is the subject of current work.

The aims of the present work are to further develop the spherical cell model, and in particular to investigate the effect of the properties of the rubber particle on the stress distributions. As discussed above, this is an important step in the development of a model to describe the toughening mechanisms and to predict the toughness of these multiphase materials. Of particular interest in the present work is the effect of the values assumed for the Young's and bulk moduli of the rubber phase, which are related through the Poisson's ratio, ν, of the rubber. It should be noted that in many rubber-toughened thermosetting polymers the rubber particles are formed via *in-situ* polymerization and phase separation processes. It is therefore not possible to measure directly and independently the moduli of the rubber particles which are formed, and an estimate of these properties is usually made via indirect measurements.

2. The finite-element model

The modelling is based on the idea of a representative cell of material containing a single sphere of rubber. The spherical material model is therefore used, and this model reflects the overall isotropy of the material. Thus, the finite element grid consists of a sphere of rubber surrounded by an annulus of epoxy polymer. This cell can be drawn using axisymmetric elements; 8-noded fully integrated elements were used except at the apex where the elements are 6-noded triangles. A typical finite-element grid is shown in Fig. 1. Analyses are also undertaken assuming a hole, instead of the rubber particle; the grid then consisted of the epoxy annulus alone. The finite-element code used was 'ABAQUS' which was run on a Convex C3800 computer.

Results have been obtained for a wide range of volume fraction of rubber spheres, up to about 40 %. The detailed investigations of the effects of the precise properties of the rubber on the calculated stress distributions were undertaken for a material containing 20 % volume fraction of rubber, since this is a typical

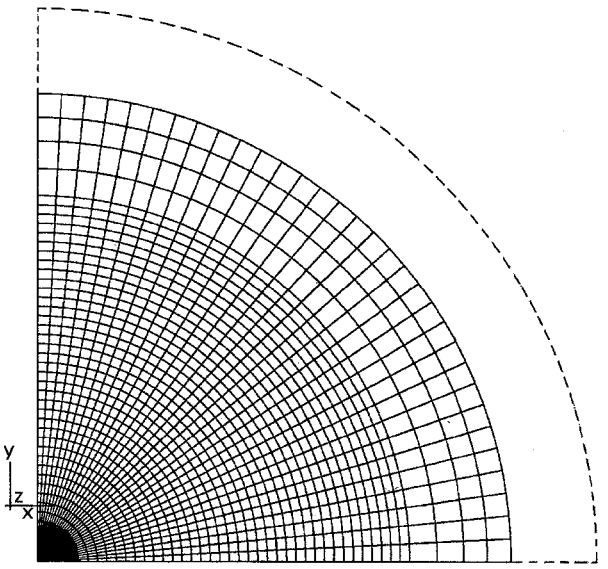

Figure 1 Typical finite-element grid showing the undeformed grid (solid lines) and the exaggerated shape of the deformed grid (dashed lines).

amount used in commercial rubber-toughened epoxy polymers.

The toughening mechanisms described above are observed ahead of a crack, in a triaxial stress field. The simplest triaxial stress field which can be applied to the spherical cell is a pure hydrostatic tensile stress. This stress field can be directly imposed via the application of stress, without the knowledge of the material properties of the overall material. The shape of the deformed grid is automatically spherical, as shown in Fig. 1, and this is the correct deformed shape. This loading was used for the detailed investigation of the effects of the rubber properties.

However, it should be noted [14] that the stress system at the crack tip under plane-strain conditions is more accurately modelled via lower stresses in the x- and z-directions (as defined in Fig. 1). To maintain the axisymmetry, the stresses in the x- and z-directions were assumed to be equal. The effects of lower stresses in the x- and z-directions were investigated via application of four stress systems: 100 MPa applied in the y-direction and 90, 80, 70 or 60 MPa applied in the x- and z-directions. However, these stress systems cannot be simply applied to the spherical cell. The overall shape of the deformed cell must remain a perfect ellipse, since the overall material is isotropic. This shape would not be attained from application of the load above; constraints must be applied to force this shape. The application of these constraints models the interactions between neighbouring spheres, see Guild and Kinloch [13]. This is analogous to the constraints applied to force the edges of the cylindrical model to remain straight. Thus, the overall properties of the material must be found by using an iterative procedure, and then loads can be applied via application of prescribed displacements to the nodes around the edge of the grid. This is a lengthy procedure. The complex loading systems were applied for the grid representing 20 % volume fraction of rubber particles and for one set of properties of the rubber particle, namely with $E = 1$ MPa and $\nu = 0.49992$, and for a hole.

3. Material properties

The results presented in the present paper are for linear elastic properties and input values of Young's modulus, E, and Poisson's ratio, ν, are needed. The values used are shown in Table I. The values for a typical epoxy matrix polymer are well established. However, as commented above, the value of the Young's modulus, E, of the rubbery phase is far more difficult to establish and the range of values taken reflects the values quoted in the literature [15] where the *in-situ* polymerization has been simulated to manufacture 'bulk' specimens of the rubber particles, which were subsequently used to determine the value of E from tensile stress versus strain measurements. A sensible range of Poisson's ratio, ν, for the rubber has been selected. The upper value chosen for ν is very close to the maximum theoretical value of 0.5. It should be noted that the finite-element analysis package which has been employed fails if the value of $\nu = 0.5$ is used. However, the maximum value of ν used in the present work is higher than that used previously by Huang and Kinloch [5, 6, 16] and Guild and Young [11]. Such relatively high values may now be used due to improved precision of the finite-element analysis code.

The major, and most important, advantage of being able to use relatively high values for the Poisson's ratio is that this implies that the bulk modulus, K, of the rubber particle is relatively high. Indeed, input values E of 1 MPa and $\nu = 0.49992$ imply a value of K of about 2 GPa, which is of the order expected for a rubbery polymer [17]. Thus, also indicated in Table I are the values of the bulk modulus, K, and the shear modulus, G, which may be derived from the input properties of the Young's modulus, E, and Poisson's ratio, ν.

The ranges of the values of the bulk modulus, K, and the shear modulus, G, of the rubbery phase, which may be derived from the input values of Young's modulus, E, and Poisson's ratio, ν, are also shown in Fig. 2. As expected, of course, for a given input value of E, the value of the shear modulus, G, is relatively

TABLE I Material properties

Phase	Input properties		Derived properties	
	E(GPa)	ν	K(GPa)	G(GPa)
Epoxy	3.0	0.35	3.333	1.111
Rubber	0.001 to 0.003	0.490 to 0.49999	0.0167 to 6.0	0.000333 to 0.001

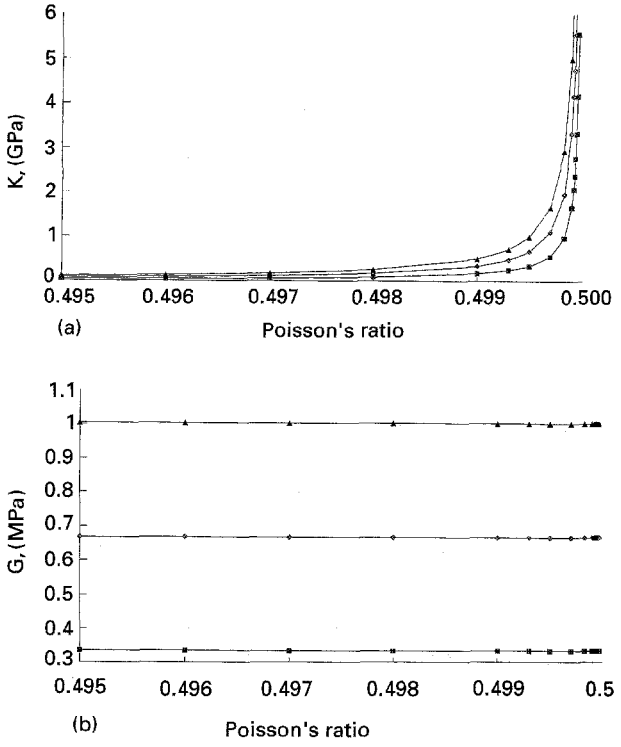

Figure 2 Variation of derived properties of the rubber phase as a function of the input properties. (a) Variation of bulk modulus, K, with Poisson's ratio, ν, for different values of Young's modulus, E. (b) Variation of shear modulus, G, with Poisson's ratio, ν, for different values of Young's modulus, E. —■— E = 1 MPa, —◆— E = 2 MPa —▲— E = 3 MPa.

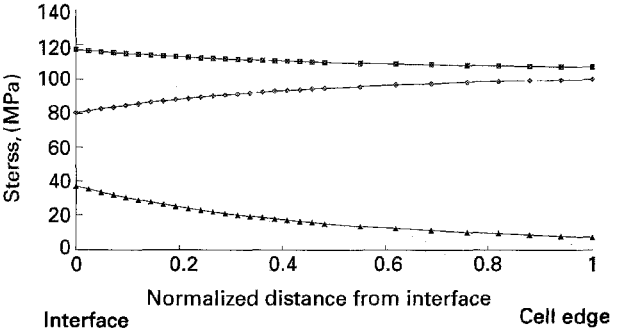

Figure 3 Stress profiles through the epoxy annulus for an applied pure hydrostatic tension of 100 MPa. (Volume fraction of rubber phase is 20%; rubber properties are: E = 1 MPa and ν = 0.4999.) —■— Tangential stress —◆— Radial stress —▲— Von Mises stress.

insensitive to the input value of ν. On the other hand, for a given input value of E, the value of the bulk modulus, K, is extremely sensitive to the precise value of ν, when ν is greater than about 0.499.

The effect of simply having a void, or hole, in the epoxy cell has also been ascertained. This was undertaken so that the effect of a cavitated, or interfacially debonded, rubber particle could be studied. As noted above, this aspect is of importance in the toughening process, as it subsequently allows plastic hole-growth in the epoxy matrix to occur.

4. Results

4.1. Overall stress distribution

The overall features of the stress distribution were unchanged for the range of rubber properties employed. Application of a pure hydrostatic tensile stress to the representative cell places the rubber sphere in uniform hydrostatic tension. The stresses within the epoxy annulus vary, but are radially symmetric as expected. The maximum direct stress is at the interface, in the tangential direction, and the maximum von Mises equivalent stress is also at the interface. The radial stress is a maximum at the outer surface of the epoxy annulus. Typical profiles through the epoxy annulus for the direct (tangential), radial and von Mises stresses are shown in Fig. 3. These profiles are for 20 % volume fraction of rubber particles with the properties of the rubber being taken as E = 1 MPa and ν = 0.4999; thus giving a value of K for the rubber of 1.67 GPa. The imposed hydrostatic stress was generated by applying a pure hydrostatic tensile stress of 100 MPa, that is, with the stresses acting in any direction being 100 MPa. This gives rise to a maximum tangential stress of about 118 MPa at the rubber/epoxy interface, and a maximum von Mises stress of about 35 MPa also at this location. The maximum radial stress is at the surface of the epoxy annulus and has a value of 100 MPa, which is equal to the imposed applied hydrostatic stress, as required. At the rubber/epoxy interface, the radial stress is equal to the hydrostatic stress in the rubber particle, and has a value of about 80 MPa.

4.2. Effect of volume fraction of rubbery phase

The effects of the stress distributions arising from varying the volume fraction of the rubbery phase have been deduced using a constant value of Young's modulus of the rubber of E = 1 MPa. Two values of Poisson's ratio, ν, have been used; namely ν = 0.490 and ν = 0.49992. These values give bulk moduli, K, for the rubber particle of about 0.02 GPa and 2 GPa, respectively. As commented above, the relatively high value of ν = 0.49992 gives a bulk modulus value of about 2 GPa, which is considered to be the more appropriate for a rubbery polymer. Also, stress distributions arising from simply having a hole present in the epoxy cell were studied. In all cases the applied stress was pure hydrostatic tension of 100 MPa.

The application of hydrostatic stress leads to values of only the bulk modulus of the cell; the complete elastic properties can only be found from unidirectional loading. The variation of the bulk modulus of the representative cell (i.e. the bulk modulus of the rubber-toughened epoxy) is shown as a function of the volume fraction of the rubber phase in Fig. 4. For a value of ν = 0.49992 for the rubber particle, the bulk modulus of the rubber-toughened epoxy is relatively high and is not greatly dependent upon the volume fraction of the rubber particle. In contrast, when the value of ν = 0.490 is taken for the rubber particle, the bulk modulus of the rubber-toughened epoxy is relatively lower and is very dependent upon the volume fraction of the rubber

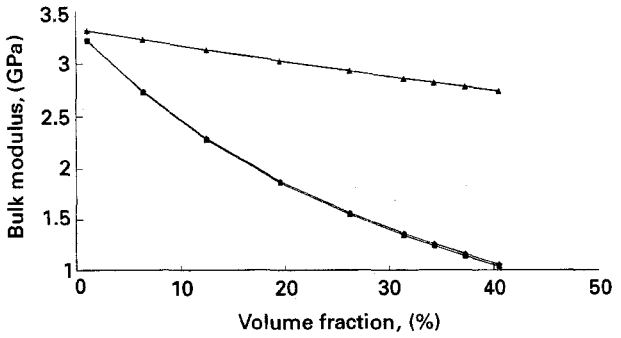

Figure 4 Variation of the bulk modulus of the rubber-toughened epoxy with volume fraction of rubber phase for different values of Poisson's ratio, ν, of the rubber particle, and a hole. (Applied pure hydrostatic tension of 100 MPa; rubber properties are: E = 1 MPa.) —■— Hole —◆— Poisson's ratio = 0.490 —▲— Poisson's ratio = 0.49992.

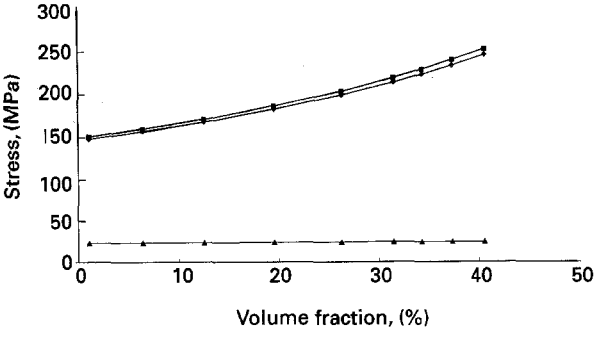

Figure 6 Variation of the maximum von Mises stress in the epoxy matrix with volume fraction of rubber phase for different values of Poisson's ratio, ν, of the rubber particle, and a hole. (Applied pure hydrostatic tension of 100 MPa; rubber properties are: E = 1 MPa.) —■— Hole —◆— Poisson's ratio = 0.490 —▲— Poisson's ratio = 0.49992.

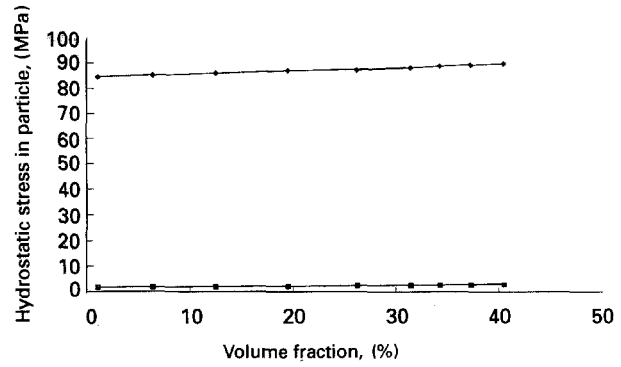

Figure 5 Variation of the hydrostatic tensile stress in the rubber particle with volume fraction of rubber phase for different values of Poisson's ratio, ν, of the rubber particle. (Applied pure hydrostatic tension of 100 MPa; rubber properties are: E = 1 MPa.) —■— Poisson's ratio = 0.490 —◆— Poisson's ratio = 0.49992.

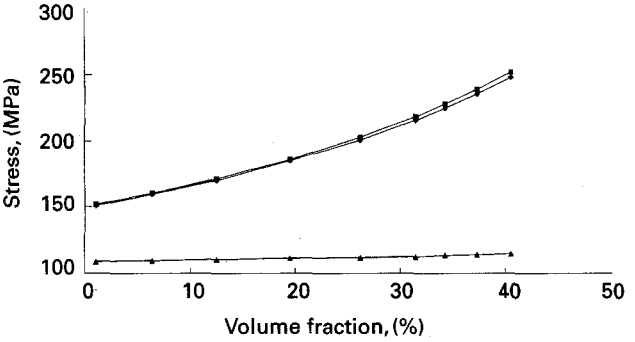

Figure 7 Variation of the maximum direct (tangential) stress in the epoxy matrix with volume fraction of rubber phase for different values of Poisson's ratio, ν, of the rubber particle, and a hole. (Applied pure hydrostatic tension of 100 MPa; rubber properties are: E = 1 MPa.) —■— Hole —◆— Poisson's ratio = 0.490 —▲— Poisson's ratio = 0.49992.

particle. Further, when ν for the rubber particle is 0.490, then the values for the bulk modulus of the rubber-toughened epoxy are in close agreement with those values obtained when simply a void, or hole, is assumed to exist in the epoxy matrix.

The variation of hydrostatic stress in the rubber particle is shown as a function of the volume fraction of the rubber phase, and for different values of ν of the rubber, in Fig. 5. The hydrostatic stresses for the Poisson's ratio of 0.49992 are about forty times greater compared to the stresses for the Poisson's ratio of 0.490. For both values of Poisson's ratio, the hydrostatic stress in the rubber increases slightly as the volume fraction of rubber phase increases. The hydrostatic stress being greater in the rubber particle, when its Poisson's ratio is high, would be expected, of course. This arises since a higher value of Poisson's ratio leads to a higher value of bulk modulus for the rubber particle, and hence greater hydrostatic stress levels arise.

The variations of the maximum von Mises stress and maximum direct stress in the epoxy matrix are shown in Figs 6 and 7, respectively. As shown previously in Fig. 3, for both of these types of stresses their maximum values occur at the rubber/epoxy interface. The results for the lower value of Poisson's ratio (ν = 0.490) reveal relatively high values of von Mises and direct stresses in the epoxy matrix, and these stresses increase significantly as the volume fraction of rubber phase increases. Further, these results are very similar, but not completely identical, to the results for a hole. The von Mises and direct stresses for the case when the rubber has a relatively high Poisson's ratio (ν = 0.49992) are low in magnitude and are almost independent of the volume fraction of the rubber phase. These effects arise from the stress concentrations being caused by the difference in properties between the rubber sphere and epoxy annulus. Hence, increasing the value of the Poisson's ratio of the rubber decreases this difference, so the stress concentrations would be expected to be smaller.

4.3. Effects of rubber properties

The effect of the precise rubber properties has been investigated in detail for a volume fraction of 20 % of rubber phase. As indicated in Table I, analyses were undertaken for a range of Young's modulus, E, of the rubber and as a function of the Poisson's ratio, ν, of the rubber. The predicted variations of the bulk modulus of the rubber-toughened epoxy (i.e. the bulk modulus for the representative cell) are shown in

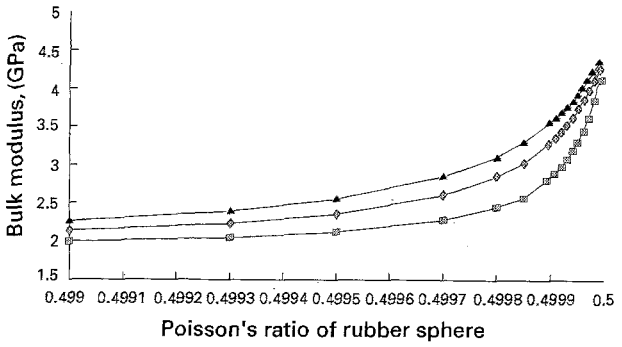

Figure 8 Variation of the bulk modulus of the rubber-toughened epoxy with Poisson's ratio, ν, of the rubber particle for different values of the Young's modulus, E, of the rubber. (Applied pure hydrostatic tension of 100 MPa; volume fraction of rubber is 20%.) —■— E = 1 MPa —◆— E = 2 MPa —▲— E = 3 MPa.

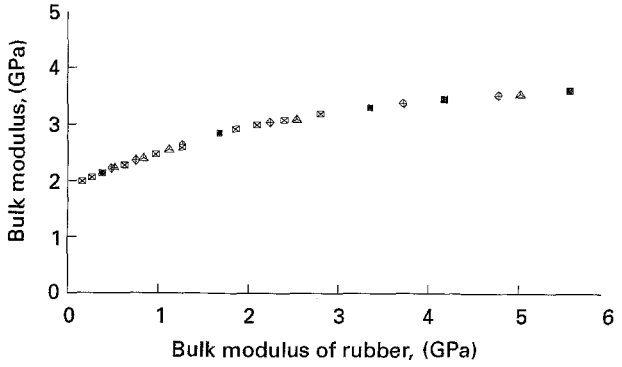

Figure 9 Variation of the bulk modulus of the rubber-toughened epoxy with bulk modulus, K, of the rubber particle for different values of the Young's modulus, E, of the rubber. (Applied pure hydrostatic tension of 100 MPa; volume fraction of rubber is 20%.) ⊠E = 1 MPa ⊕ E = 2 MPa △E = 3 MPa.

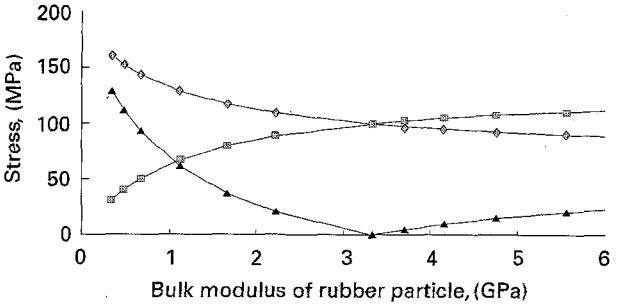

Figure 10 Variation of the different types of maximum stresses with bulk modulus, K, of the rubber particle. (Applied pure hydrostatic tension of 100 MPa; volume fraction of rubber is 20%.) —⊠— Hydrostatic stress in rubber (MPa) —⊕— Maximum direct stress in epoxy (MPa) —▲— Maximum von Mises stress in epoxy (MPa).

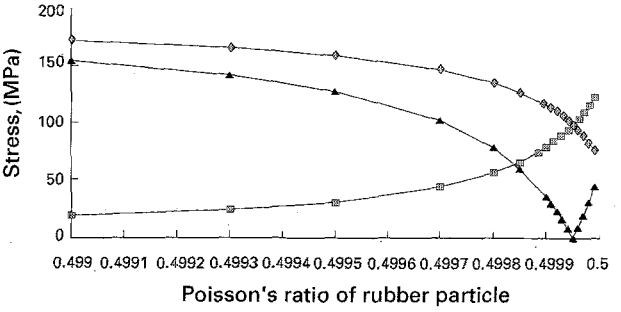

Figure 11 Variation of the different types of maximum stresses with Poisson's ratio, ν, of the rubber particle. (Applied pure hydrostatic tension of 100 MPa; volume fraction of rubber is 20%; rubber properties are: E = 1 MPa.) —⊠— Hydrostatic stress in rubber (MPa) —⊕— Maximum direct stress in epoxy (MPa) —▲— Maximum von Mises stress in epoxy (MPa).

Fig. 8, and the value approximately doubles over the range studied. As may be seen, the predicted value increases sharply for relatively high values of Poisson's ratio of the rubber. As expected, this coincides with the sharp increase in the change of bulk modulus of the rubber, as shown in Fig. 2a.

From the values of the Young's modulus, E, and Poisson's ratio, ν, employed for the rubber in the above calculations one may obviously deduce the bulk modulus, K, of the rubber. Therefore, the predicted values of the bulk modulus of the rubber-toughened epoxy (i.e. K for the representative cell) are plotted against the value of K for the rubber in Fig. 9. The values for all the different analyses fall onto one relationship. Thus, the value of the bulk modulus of the rubber-toughened epoxy is dependent only upon the bulk modulus, K, of the rubber, the volume fraction of the rubbery phase and the properties of the epoxy matrix being held constant; see Table I. This observation was also recorded for all the different types of stress distributions when they were calculated as functions of the Young's modulus, E, and Poisson's ratio, ν, of the rubber. Namely, the predicted values of stresses are unique functions of the bulk modulus of the rubber particle, the volume fraction of the rubbery phase and the properties of the epoxy matrix again being held constant. This is discussed in more detail below; see Fig. 10.

Of course, the bulk modulus of the rubber-toughened epoxy material is not dependent upon the type of applied stress system. Also, as noted above, when pure hydrostatic tension is applied to the cell the predicted values of stress distributions are unique functions of the bulk modulus of the rubber particle. However, it should be noted that this observation for the stress distributions is only appropriate to the applied stress system of pure hydrostatic stress. Preliminary results for unidirectional loading imply a more complex relationship between the stress distributions and the properties of the rubber, i.e. the values of E and ν (and hence E and K) of the rubber. Thus, for the 'crack-tip' applied stress systems used in the present work, and described below in Section 4.4, the stress distributions in the rubber-toughened epoxy material are *not* uniquely defined by the bulk modulus of the rubber particle, even when the volume fraction of the rubbery phase and the properties of the epoxy matrix are held constant. The relationships for the directional applied stress systems are discussed in detail elsewhere [18].

The variations in the (i) hydrostatic stress in the rubber particle, (ii) maximum von Mises stress in the epoxy matrix, and (iii) maximum direct stress in the epoxy matrix are shown as a function of the bulk modulus, K, of the rubber phase in Fig. 10. These

results are for pure hydrostatic tensile stresses being applied to the cell and, as discussed above, they fully describe the variability of the different types of maximum stresses with respect to the properties of the rubber phase. Fig. 11 shows the results for a fixed value of the Young's modulus, E, of the rubber of 1 MPa and the variations in the stresses are shown as a function of the Poisson's ratio of the rubber particle. These results further emphasize the very great dependence of the values of the maximum stresses on the Poisson's ratio, for high values of Poisson's ratio.

The results in Fig. 10 demonstrate that the hydrostatic stress in the rubber sphere increases steadily with increasing bulk modulus of the rubber, although the rate of increase is lower as the value of K for the rubber rises. When the value of K of the rubber equals that of the epoxy annulus (i.e. equals 3.333 GPa), the model responds as an isotropic sphere and the stress state is pure hydrostatic tension. The maximum direct stress in the epoxy annulus decreases steadily with increasing bulk modulus of the rubber, although the rate of decrease is lower as the value of K for the rubber rises. The maximum von Mises stress in the epoxy annulus decreases relatively rapidly with increasing bulk modulus of the rubber, and attains a value of zero when the value of K of the rubber equals that of the epoxy. Since values of the von Mises stress are always positive, at higher values of K of the rubber the von Mises stress increases gradually as the value of K for the rubber continues to rise.

4.4. Effect of applied stress system

The effect of non-uniform stress systems has been studied for a volume fraction of 20 % of rubber particles, or holes. The rubber particles had properties of $E = 1$ MPa and $\nu = 0.49992$, thus implying a bulk modulus of the rubber of K of about 2 GPa. Results were obtained for four different stress systems; the y-direction stress was set at 100 MPa, and the x- and z-direction stresses were varied.

The overall stress system distributions were in agreement with the previous results for the pure hydrostatic tensile stress system; see Fig. 3. The rubbery particle was always placed in uniform hydrostatic tension and the maximum concentrations of radial and von Mises stresses in the matrix were found at the equatorial plane of the particle, again at the particle/matrix interface. The results are shown in Table II, and are compared with the results for the pure hydrostatic tension loading system.

Now, as the stresses in the x- and z-directions are reduced, the applied pure hydrostatic tensile stress to the cell is reduced but the deviatoric (i.e. pure shear) component of the stress tensor will increase. Also, as the stresses in the x- and z-directions are reduced, the direct strain in the y-direction will increase. Thus, several major changes in the stresses and strains experienced by the cell occur as the applied stress system is changed.

Considering firstly the results for the epoxy matrix containing a hole, then as the stresses in the x- and z-directions are reduced the maximum von Mises stress in the epoxy slightly decreases and the maximum direct stress in the epoxy slightly increases. However, these changes are not very significant when compared with those seen in the rubber-toughened epoxy material. Secondly, as the stresses in the x- and z-directions are reduced for the rubber-toughened epoxy, the hydrostatic stress in the rubber particle decreases. However, all the other values of the stresses increase as the asymmetry of the loading increases. For example, the von Mises stress in the epoxy matrix increases by a factor of about three as one goes from an applied stress system of 100:100:100 MPa to 100:60:60 MPa. Thus, the simple use of an applied pure hydrostatic stress system to model the conditions ahead of a crack lead to significantly reduced predictions for the values of the maximum von Mises stresses in the epoxy matrix compared to more realistic 'crack-tip' stress state systems.

A final point of interest is that the rubber particle is placed in virtually pure hydrostatic tension for all the stress systems used in the present work, including the asymmetric systems. This result may be compared with the stress state of the rubbery phase under a unidirectional tensile load. For both single-phase particles [11] and multiphase particles [12] the rubbery phase has again been found to be in virtually pure hydrostatic tension. The ability of the rubbery phase to achieve this stress state must arise from the fact

TABLE II Effect of stress system

Applied stress y:x:z (MPa)	Hydrostatic stress in the rubber (MPa)	Max. direct stress in the epoxy (MPa)	Max. von Mises stress in the epoxy (MPa)
Rubber particle			
100:100:100	87.1	111.3	24.1
100:90:90	81.3	118.8	32.4
100:80:80	75.5	126.2	44.6
100:70:70	69.7	133.7	58.4
100:60:60	63.9	141.2	72.7
Void			
100:100:100	–	187.7	187.4
100:90:90	–	190.0	181.9
100:80:80	–	192.4	177.7
100:70:70	–	194.8	174.8
100:60:60	–	197.2	173.3

that, although it possesses a high bulk modulus, it has an extremely low shear modulus. Also, it should be noted that all the analyses have been conducted using small deformation theory. The shape of the deformed grid is therefore not taken into account in the stress calculations. The extension of this work to include the effect of high deformations is currently in progress.

5. Discussion

We have investigated the stress distributions in and around a rubber particle in a matrix of epoxy polymer, and also deduced the bulk modulus of the rubber-toughened epoxy. Of particular concern has been the effects of the volume fraction and the properties of the rubber phase. The Young's modulus, E, and Poisson's ratio, ν, of the rubber phase have been varied, so changing the bulk modulus, K, of the rubber; see Fig. 2. The properties of the epoxy matrix have been kept constant; see Table I. Many interesting discussion points arise from the results reported in the previous sections.

As shown in Figs 5, 6 and 7, the volume fraction of the rubbery phase (or hole) does influence the level of stresses generated both in the rubber particle and in the epoxy matrix. However, the volume fraction of the rubber particles may be readily measured, and controlled, and hence the information given in these figures may be directly employed in a predictive model.

The predicted bulk modulus of the rubber-toughened epoxy is shown as a function of the volume fraction of rubber particles in Fig. 4, the Poisson's ratio of the rubbery particles in Fig. 8 and the bulk modulus of the rubber particle in Fig. 9. (Recall the interrelationship between the Poisson's ratio and the bulk modulus of the rubber particle shown in Fig. 2a.) Firstly, the unique relationship between the predicted bulk modulus of the rubber-toughened epoxy and the bulk modulus of the rubber particle, shown in Fig. 9, should be noted. Secondly, experimental values of the bulk modulus of the rubber-toughened epoxies are not reported in the literature. However, values of the tensile modulus and shear modulus have been reported [3, 19] as a function of volume fraction. Hence, the Poisson's ratio and the bulk modulus of the material may be deduced as a function of volume fraction. For a volume fraction of about 20 % rubber particles, the decrease in bulk modulus of the material would be expected from such experimental data to be about 10 to 15 %. From Fig. 4, for a $\nu = 0.49992$ (giving a K of rubber particles of about 2 GPa) the predicted decrease in bulk modulus of the material is about 10 %. Hence, there is very good agreement between theory and experiment.

The choice of the bulk modulus, K, of the rubber phase (as fixed by the input values of E and ν for the rubber) has a significant effect on the level of stresses generated both in the rubber particle and in the epoxy matrix. Fig. 10 illustrates how the levels of all the different types of stress concentrations are dependent upon the value of the bulk modulus of the rubbery particles; for example, whether K of the rubber phase is taken to be 1 or 3 GPa has a major effect. This is I1a very important observation, since, as commented previously, it is often difficult to ascertain the value of the bulk modulus (or Poisson's ratio) of the rubber phase with great precision. Hence, the uncertainty in the values of the stress distributions may present problems in further quantitative modelling of the toughening mechanisms. It is also noteworthy that for the application of a pure hydrostatic tensile stress, the stress distributions, and bulk modulus of the rubber-toughened epoxy, are uniquely dependent upon the value of the bulk modulus of the rubber phase, the volume fraction of the rubbery phase and the properties of the epoxy matrix being held constant.

As previously commented by Huang and Kinloch [16, 20], the precise value of the bulk modulus, K, (or Poisson's ratio, ν) of the rubber particle will have a major influence on the exact sequence of the toughening mechanisms. For example, Figs 10 and 11 clearly reveal that a relatively low value of K (or ν) of the rubber will tend to lead to relatively low hydrostatic stresses in the rubber, but high von Mises stresses in the epoxy. Thus, this will tend to promote shear yielding in the epoxy in preference to cavitation (or debonding) in the rubber particle it is also of interest to note that any particle with a relatively low bulk modulus (e.g. a polyethylene particle) would also obviously promote such shear yielding. However, low bulk-modulus particles give rise to relatively low hydrostatic stresses, and therefore they would not tend to readily cavitate, or debond. Recall that the importance of cavitation, or debonding, of the particle is that this gives rise to void formation which may then enable subsequent plastic hold growth in the epoxy to occur, and plastic hole growth in the epoxy matrix is a major toughening mechanism. On the other hand, a relatively high value of K (or ν) of the particle will tend to lead to relatively high hydrostatic stresses in the particle, but low von Mises stresses in the epoxy. Thus, in this case, cavitation of the rubber particle will first be initiated, in preference to shear yielding of the epoxy matrix. As discussed in more detail below, a further point to note in this respect is that cavitation of the rubber particle will lead to a void and, from Figure 6, it may be seen that, for a rubber with a relatively high value of ν (or K), this will lead to a considerable increase in the von Mises stress in the epoxy matrix. Thus, extensive shear yielding and plastic hole growth in the epoxy matrix are both relatively favoured toughening mechanisms once void formation in the particle has occurred.

To expand the above discussion, with the rubber having a bulk modulus of about 2 GPa (for example, if E = 1 MPa and $\nu = 0.49992$; giving a K of about 2 GPa) then from Figs 5, 6 and 10 (or 11) it would be expected that cavitation will precede the initiation of localized shear bands, but once cavitation has occurred (and hence a void has been created) the von Mises stress will rise dramatically and readily lead to plastic shear band formation and plastic hole-growth in the epoxy matrix. This observation is in good agreement with the results reported by Parker *et al.* [21]. These workers employed rubber particles which were preformed before being added to a polycarbonate matrix and, from subsequent fracture experiments, they concluded that cavitation preceded localized

shear yielding. The pure rubbery particles they employed would possess a Poisson's ratio approaching 0.5 and the observed sequence of events would be as predicted by our finite-element modelling. In the case of rubber-toughened epoxy polymers the situation is complicated by the fact that the value of ν of the rubber particle will be dependent upon the amount of epoxy matrix trapped inside the particles, since the particles form by *in-situ* polymerization and phase separation processes. Consequently, the exact sequence of initiation of the two mechanisms could be different for different formulations of rubber-toughened epoxy polymers. However, certainly the most detailed studies that have been reported [4, 22] suggest that cavitation precedes localized shear yielding.

The question of whether an important role of voiding of the rubber particle, due to either cavitation or debonding, is to relieve the triaxial constraint at the crack tip has been raised in the literature [1, 2, 22]. This effect is equivalent to the formation of a series of holes, or voids, greatly reducing the degree of triaxial tensile stresses acting in the matrix, and thereby promoting plastic yielding in the matrix. As discussed above, the precise value of the bulk modulus, K, (or Poisson's ratio, ν) of the rubber particle will have a major influence on the answer to this question. If the Poisson's ratio, ν, of the rubber particle is relatively low, then any cavitation, or debonding, to form a hole would not significantly change the von Mises stress in the epoxy matrix; see Fig. 6. However, if the Poisson's ratio, ν, of the rubber particle is relatively high, then any cavitation, or debonding, to form a hole would indeed greatly increase the von Mises stress in the epoxy matrix, thus effectively relieving the triaxial constraint; again see Fig. 6. In this case cavitation or debonding would significantly promote any form of plastic shear yielding mechanism.

This above conclusion obviously implies that small, well-dispersed holes should also significantly toughen an epoxy polymer, and indeed this has recently been shown to be the case [7]. However, the introduction of holes into an epoxy during the curing process is not easy, compared to the relatively straightforward attainment of a rubber-particulate microstructure which may later debond or cavitate when the material is loaded to give a "holes" ahead of the crack tip. Also, of course, the initial presence of holes throughout the complete body of the material will lead to the loss of other important properties, such as water resistance and permability coefficient.

Finally, the results shown in Table II demonstrate that the exact details of the stress system applied to the cell are important. For example, for the rubber-toughened epoxy, the hydrostatic stress in the rubber decreases somewhat but the maximum von Mises stress in the matrix increases greatly as the stress system becomes more asymmetric in nature. The slight decrease in the hydrostatic tensile stress in the rubber may somewhat inhibit the cavitation or debonding of the rubber but, on the other hand, the major increase in the von Mises stress in the epoxy matrix may significantly aid the initiation and growth of shear bands.

6. Conclusions

Predictive modelling of rubber-toughened epoxy polymers is a powerful tool for the investigation of the failure mechanisms. The importance of the rubber properties has been highlighted and it has been shown that the exact nature of these properties may influence the sequence of failure events in the material. The precise material properties of the rubbery phase in the rubber-toughened epoxy cannot be directly measured. However, a likely range of properties for the rubbery phase has been assumed and a comparison between the predicted and experimentally measured bulk properties of the rubber-toughened epoxy reveals good agreement. Thus, the importance of the different failure micromechanisms, and the sequence in which they occur, can be assessed. Hence, the quantitative prediction of toughening mechanisms in such materials may now be more readily undertaken.

Acknowledgements

The authors gratefully acknowledge valuable discussions with Dr B. A. Crouch, E. I. Du Pont, Dr D. L. Hunston, NIST; and Professor A. F. Yee, University of Michigan. The computer time used in the present work is supported by a grant from the Engineering and Physical Sciences Research Council.

References

1. A. J. KINLOCH, in "*Rubber-toughened plastics*", edited by C. K. Riew (Advances in Chemistry Series **222**, American Chemical Society, Washington DC, 1989) p. 67.
2. A. J. KINLOCH, S. J. SHAW and D. L. HUNSTON, *Polymer* **24** (1983) 1355.
3. A. F. YEE and R. A. PEARSON, *J. Mater. Sci.* **21** (1986) 2462.
4. R. A. PEARSON and A. F. YEE, *ibid* **21** (1986) 2475.
5. Y. HUANG and A. J. KINLOCH, *ibid* **27** (1992) 2753.
6. *Idem*, *ibid* **27** (1992) 2763.
7. *Idem*, **33** (1992) 1330.
8. L. J. BROUTMAN and G. PANIZZA, *Int. J. Polym. Mat.* **1** (1971) 95.
9. B. D. AGARWAL and L. J. BROUTMAN, *Fibre Sci. Tech.* **7** (1974) 63.
10. P. J. DAVY and F. J. GUILD, *Proc. Royal Soc.*, **A148** (1988) 95.
11. F. J. GUILD and R. J. YOUNG, *J. Mater. Sci.* **24** (1989) 2454.
12. F. J. GUILD, R. J. YOUNG and P. A. LOVELL, *J. Mater. Sci. Letters* **13** (1994) 10.
13. F. J. GUILD and A. J. KINLOCH, *ibid* **13** (1994) 629.
14. A. J. KINLOCH and R. J. YOUNG, "Fracture behaviour of polymers" (Applied Science Publishers Ltd, London, 1983).
15. S. C. KUNZ and P. W. R. BEAUMONT, *J. Mater. Sci.* **16** (1981) 3141.
16. Y. HUANG and A. J. KINLOCH, *J. Mater. Sci. Letters*, **11** (1992) 484.
17. J. BRANDRUP and E. H. IMMERGUT, Eds, "Polymer handbook", Vols 8 and 9 (John Wiley, New York, 1989).
18. F. J. GUILD and A. J. KINLOCH, to be published.
19. A. F. YEE and R. A. PEARSON, NASA Contractor Report 3852, 1984, NASA Langley, VA, USA.
20. Y. HUANG and A. J. KINLOCH, *Polymer* **33** (1992) 5338.
21. D. S. PARKER, H. J. SUE, J. HUANG and A. F. YEE, *ibid* **31** (1990) 2267.
22. A. F. YEE, DONGMING LI and XIAOWEI LI, *J. Mater. Sci.* **28** (1993) 6392.

Received 20 July
and accepted 11 August 1994